Towards Towards Langmuir-Blodgett films of magnetically interesting materials: solution equilibria in ambiphilic iron(II) complexes of a triazole-containing ligand

Nicholas G. White,[a] **Humphrey L. C. Feltham,**[a] **Claudio Gandolfi,**[b] **Martin Albrecht**[b] **and Sally Brooker**[a]*

Supporting Information

Scheme S1. Synthesis of 3,5-di(2-pyridyl)-4-(1H-pyrrol-1-yl)-4H-1,2,4-triazole (pldpt, 3). Reagents and conditions: (a) N2H4·H2O, reflux; (b) 2 m HCl, reflux; (c) N2H4·H2O, N2H4·H2SO4, 1,2-ethandiol, 130 °C; (d) 2,5-dimethoxytetrahydrofuran, AcOH, 1,4-dioxane, reflux.

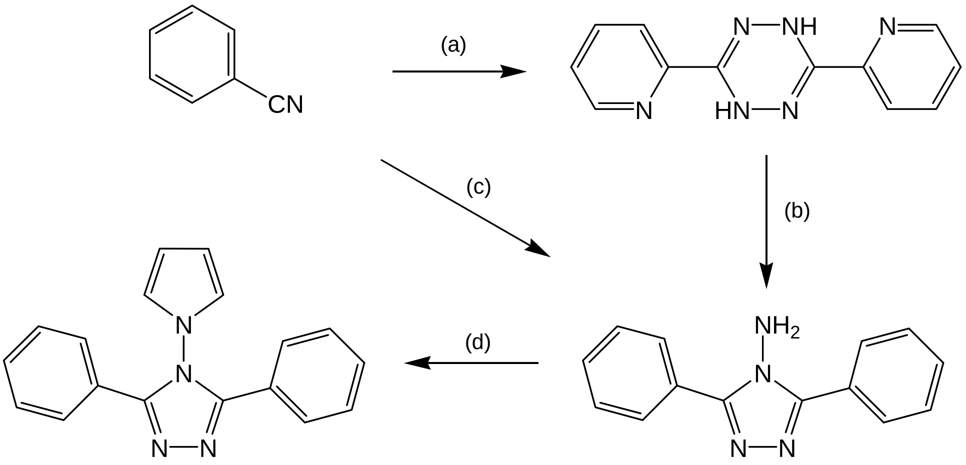

Details of attempted complexations

Initially, three equivalents of ligand were reacted with one equivalent of $[Fe^{II}(OH_2)_2(C_{16}SO_3)_2]$ in methanol, giving dark red solutions. Stirring at room temperature and then either subjecting the reaction mixture to diethyl ether vapour diffusion, or allowing it to slowly evaporate did not give [Fe(**Rdpt**)$_3$]$(C_{16}SO_3)_2$ as hoped. Instead, analytically pure [Fe(**Rdpt**)$_2$$(C_{16}SO_3)_2$] was obtained as pale orange microcrystals in reasonable yield (67% for **Rdpt** = **adpt**, 54% for **Rdpt** = **pldpt**). Attempts to carry out the reaction in different solvents were thwarted by the poor solubility of $[Fe^{II}(OH_2)_2(C_{16}SO_3)_2]$ in solvents other than methanol and water, and the poor solubility of the ligands in water.

The reaction of $[Co^{II}(OH_2)_2(C_{16}SO_3)_2]$ with either two or three equivalents of **adpt** or **pldpt** in methanol gave complexes of the form [Co^{II}(**Rdpt**)$_2$$(CH_3OH)_2$]$(C_{16}SO_3)_2$·*solvent* in good yield (77%, *solvent* = H_2O for **adpt**, 68%, *solvent* = $0.5CH_3OH$ for **pldpt**). As with the analogous iron complexes, complexes of the form $[Co^{II}(\mathbf{Rdpt})_3](C_{16}SO_3)_2$ could not be accessed, even when using three equivalents of ligand.

The starting materials $[Fe(OH_2)_2(C_{16}SO_3)_2]$ and $[Co(OH_2)_2(C_{16}SO_3)_2]$ were then reacted with *six* equivalents of **Rdpt** to see if this larger excess would allow isolation of the $[M^{II}(\mathbf{Rdpt})_3](C_{16}SO_3)_2$ complexes. The reactions with six equivalents of **pldpt** (the cobalt reaction was refluxed for 30 min to ensure all reagents dissolved; this was not a problem with the iron reaction), after vapour diffusion of diethyl ether into the reaction solution (iron) or slow evaporation of the reaction solution (cobalt), yielded $[Fe^{II}(\mathbf{pldpt})_2(C_{16}SO_3)_2]$ and $[Co^{II}(\mathbf{pldpt})_2(CH_3OH)_2](C_{16}SO_3)_2$ in similar yields and purities to the reactions with three equivalents. In the case of the reactions with six equivalents of **adpt** (again the cobalt reaction was refluxed for 30 min), the resulting complexes were found to be too soluble (on the smaller scales used) to be easily isolated by slow evaporation. Instead, vapour diffusion of diethyl ether into the reaction solutions was used. Only a small amount of $[Fe^{II}(\mathbf{adpt})_2(C_{16}SO_3)_2]$ was obtained (probably due to its high solubility; the filtrate was still highly coloured), but $[Co^{II}(\mathbf{adpt})_2(CH_3OH)_2](C_{16}SO_3)_2$ was obtained in a similar yield and purity to the reaction with three equivalents. In summary, once again it is clear that the nature of the product *isolated* from reactions of these bidentate ligands with first row transition metal ions is not controlled simply by reaction stoichiometry.

Figure S1. UV/Vis spectra of $[Fe(pldpt)(C_{16}SO_3)_2]$ in MeOH. 1:2 (**blue**) 1:3 (**maroon**) and 1:6 (**green**) ratios

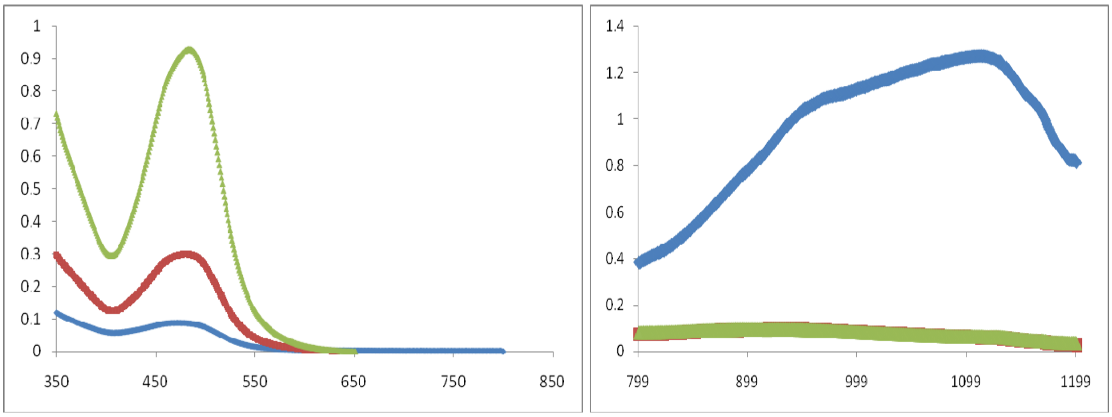

Figure S2. UV/Vis spectra of [Fe^{II}(**Rdpt**)$_2$($C_{16}SO_3$)$_2$] and [Fe^{II}(**Rdpt**)$_2$($C_{16}SO_3$)$_2$] in dichloromethane in 1:3 M:L ratios.

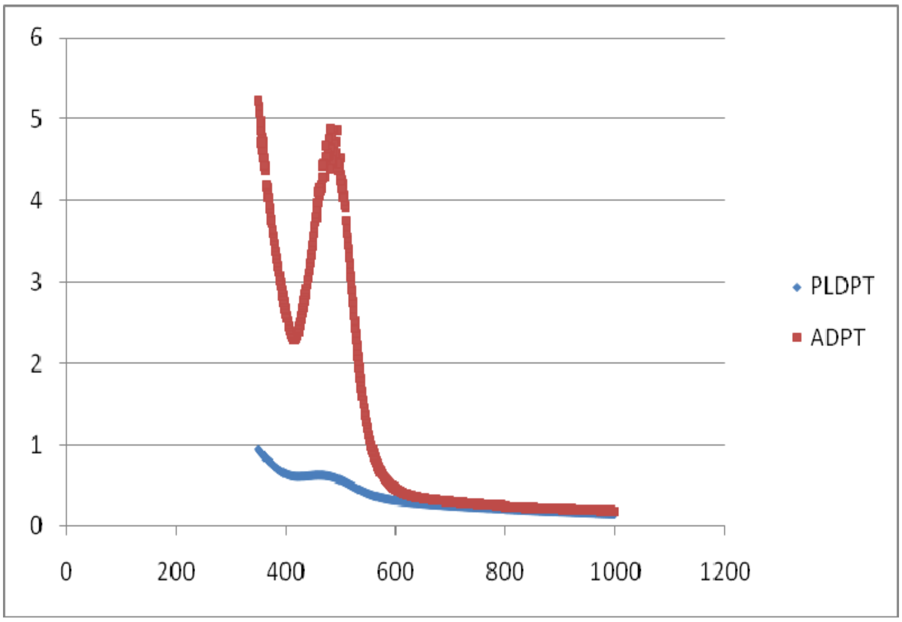

Figure S3. Pressure-area isotherms for Langmuir films prepared from [Fe^{II}(**pldpt**)$_2$($C_{16}SO_3$)$_2$] at the following concentrations: 10 nmol (red), 20 nmol (purple), 30 nmol (green), and 40 nmol (orange). At high concentrations, no liquid expanded phase was detectable anymore. identical molecular areas for all films.

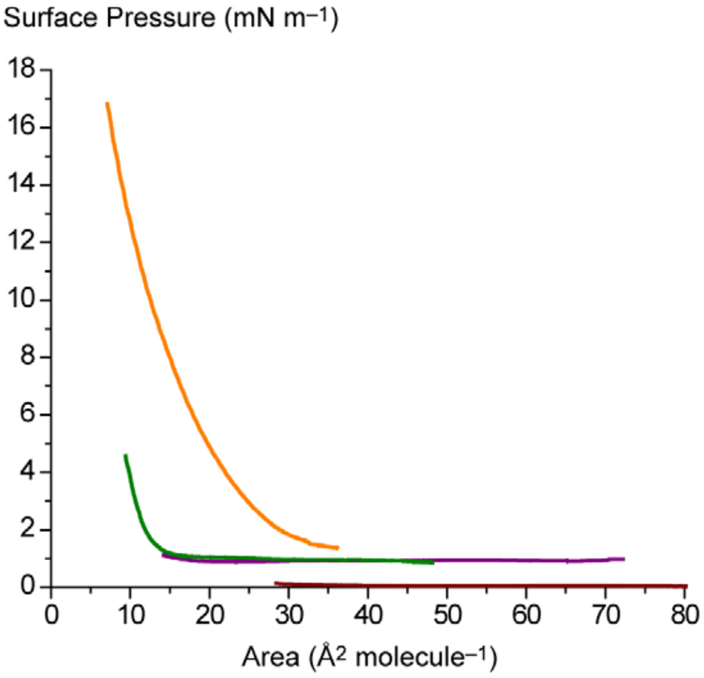

Figure S4. Pressure-time plots illustrating the low stability of the films prepared from [Fe^{II}(**pldpt**)$_2$(C$_{16}$SO$_3$)$_2$] (green), [Fe^{II}(**adpt**)$_2$(C$_{16}$SO$_3$)$_2$] (red), and Na(C$_{16}$SO$_3$) (blue).

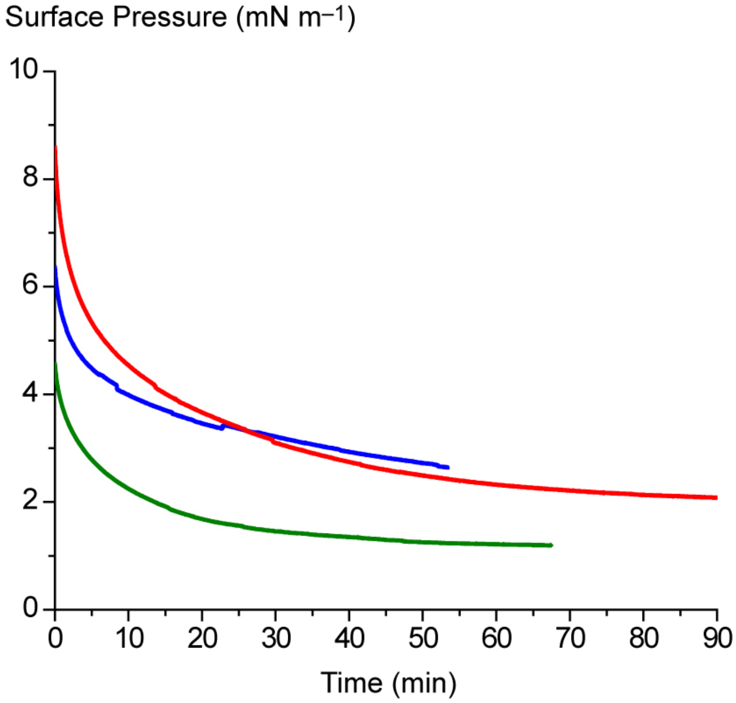

Table S1. Metal-donor bond lengths and angles.

Atoms	Bond length (Å) or angle (°)
[Fe^{II}(**adpt**)$_2$(C$_{16}$SO$_3$)$_2$]	
Fe1-O11	2.096(2)
Fe1-O21	2.101(2)
Fe1-N1 (pyridine)	2.197(3)
Fe1-N2 (triazole)	2.123(3)
Fe1-N21 (pyridine)	2.198(3)
Fe1-N22 (triazole)	2.134(3)
O11-Fe1-O21	174.64(9)
O11-Fe1-N1	94.66(9)
O11-Fe1-N2	90.33(10)
O11-Fe1-N21	86.40(9)
O11-Fe1-N22	90.63(10)
O21-Fe1-N1	90.66(9)
O21-Fe1-N2	91.57(10)
O21-Fe1-N21	88.27(9)
O21-Fe1-N22	87.47(10)
N1-Fe1-N2	75.91(10)
N1-Fe1-N21	178.91(10)
N1-Fe1-N22	104.20(10)
N2-Fe1-N21	104.35(10)
N2-Fe1-N22	179.031(11)
N21-Fe1-N22	75.52(10)
[Co^{II}(**adpt**)$_2$(CH$_3$OH)$_2$](C$_{16}$SO$_3$)$_2$·1.33CH$_3$OH	
Co1-O71	2.0682(13)
Co1-O81	2.0828(13)
Co1-N1 (pyridine)	2.1479(15)
Co1-N2 (triazole)	2.0912(15)
Co1-N21 (pyridine)	2.1512(15)
Co1-N22 (triazole)	2.1036(16)
Co2-O91	2.0697(13)
Co2-N41 (pyridine)	2.1577(15)
Co2-N42 (triazole)	2.0920(15)
O71-Co1-O81	176.11(5)
O71-Co1-N1	92.40(6)
O71-Co1-N2	92.28(6)
O71-Co1-N21	86.65(6)
O71-Co1-N22	88.70(6)
O81-Co1-N1	89.29(5)
O81-Co1-N2	84.70(6)
O81-Co1-N21	91.74(5)
O81-Co1-N22	94.38(6)
N1-Co1-N2	76.73(6)
N1-Co1-N21	178.33(6)
N1-Co1-N22	101.79(6)
N2-Co1-N21	104.67(6)
N2-Co1-N22	178.26(6)
N21-Co1-N22	76.82(6)
O91-Co2-O91a	180
O91-Co2-N41	87.11(6)
O91-Co2-N41a	92.89(6)
O91-Co2-N42	86.36(6)

O91-Co2-N42a	93.65(6)
O91a-Co2-N41	92.89(6)
O91-Co2-N41a	92.89(6)
O91a-Co2-N42	93.65(6)
O91a-Co2-N42a	86.35(6)
N41-Co2-N41a	180
N41-Co2-N42	76.79(6)
N41-Co2-N42a	103.21(6)
N41a-Co2-N42	103.21(6)
N41a-Co2-N42a	76.79(6)
N42-Co2-N42a	180

Symmetry operation used to generate equivalent atoms: a) –x+1, -y+1, -z+1.

Figure S5. Hydrogen-bonding interactions present in [Fe(**adpt**)$_2$($C_{16}H_{33}SO_3$)$_2$].

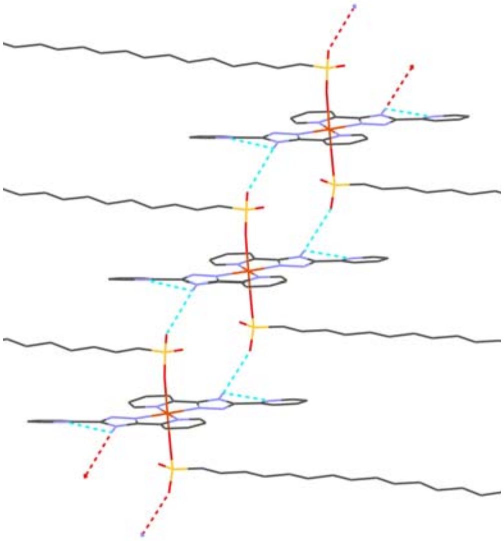

Figure S6. π-π interactions present in [Fe(**adpt**)$_2$($C_{16}H_{33}SO_3$)$_2$].

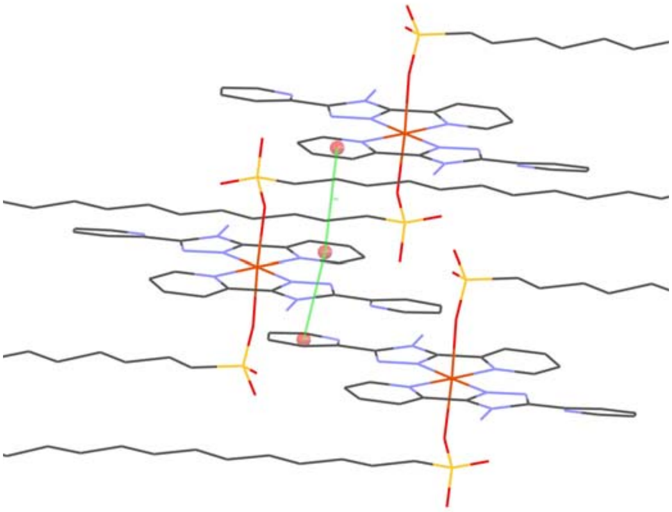

Figure S7. View of packing down *b*-axis of [Fe^{II}(**adpt**)$_2$(C$_{16}$SO$_3$)$_2$. Hydrogen atoms omitted for clarity.

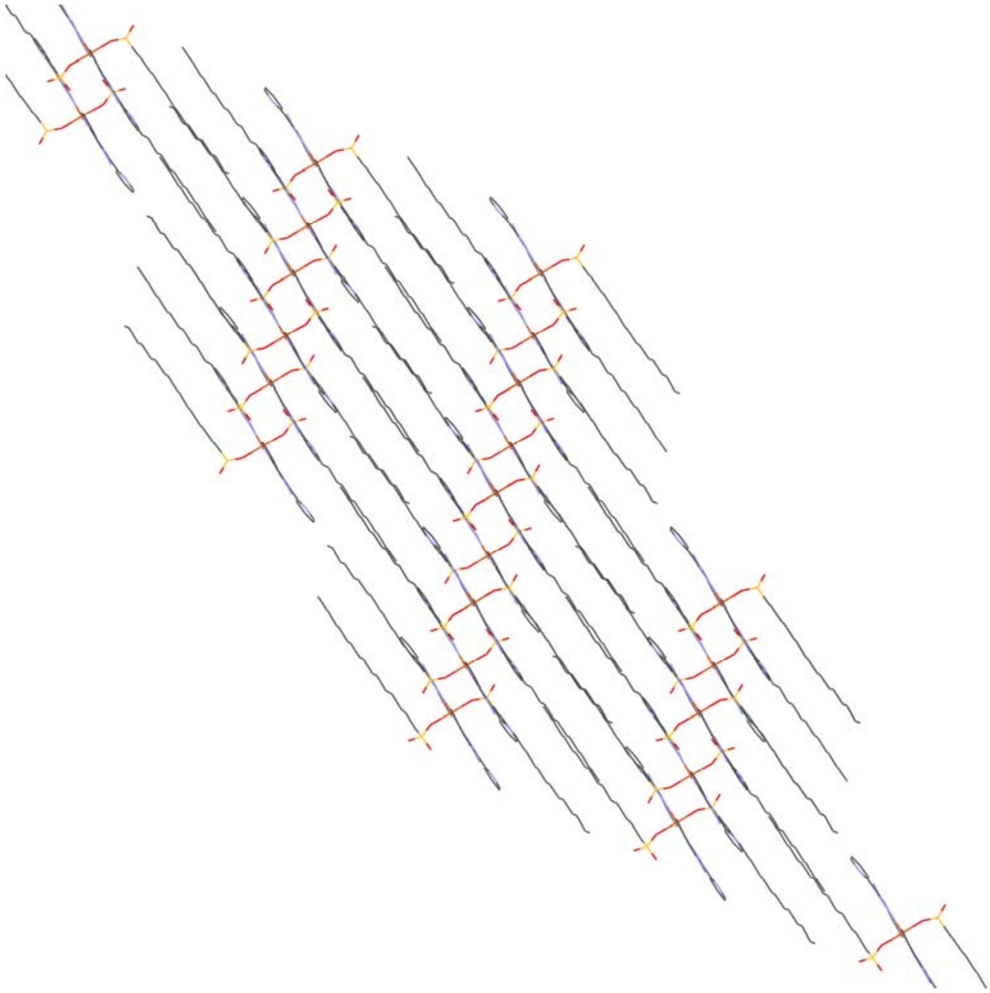

Figure S8. Hydrogen bonding (blue dashed line) and anion-π (solid green line) interactions present in [Co(**adpt**)$_2$(CH$_3$OH)$_2$](C$_{16}$SO$_3$)$_2$

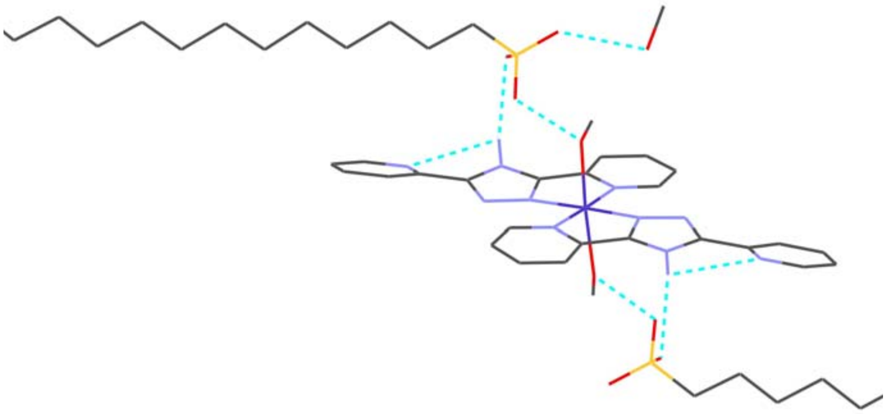

Figure S9. Packing of [Co(**adpt**)$_2$(MeOH)$_2$](C$_{16}$H$_{33}$SO$_3$)$_2$ as seen along the *a*-axis.

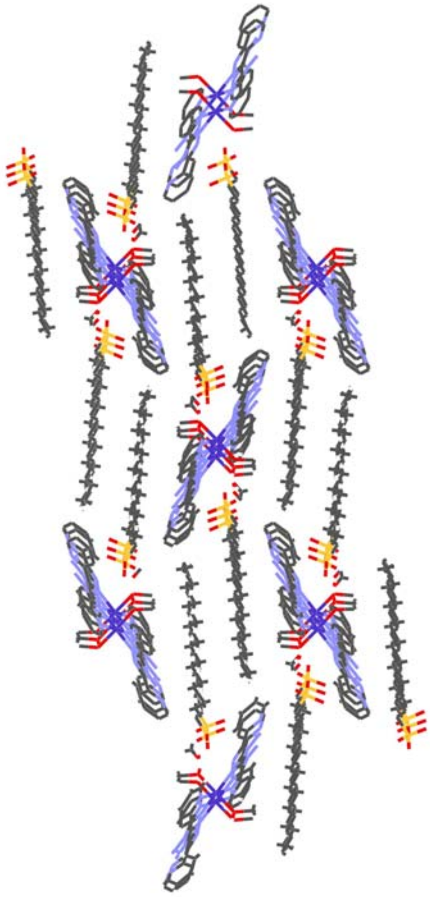

Table S2. Short hydrogen atom contacts (D…A <3.4 Å).

Atoms	D-H (Å)	H…A (Å)	D…A (Å)	<D-H…A (°)

[Fe^{II}(**adpt**)$_2$(C$_{16}$SO$_3$)$_2$]				
N6-H6x…O12_a	0.95	2.12	2.885(4)	136.6
N6-H6y…N4	0.95	2.17	2.870(4)	129.5
N26-H26x…N24	0.92	2.11	2.875(4)	139.6
N26-H26y…O22_b	0.92	2.27	2.998(4)	136.0
[Co^{II}(**adpt**)$_2$(CH$_3$OH)$_2$](C$_{16}$SO$_3$)$_2$·1.33CH$_3$OH				
N6-H6x…O13	0.90	1.98	2.849(2)	163.4
N6-H6y…N4	0.97	2.07	2.866(2)	137.6
N26-H26x…O22	0.91	2.03	2.903(2)	160.6
N26-H26y…N24	0.90	2.16	2.887(2)	137.5
N46-H46x…O32	0.88	2.17	2.861(2)	134.3
N46-H46y…N44	0.96	1.93	2.861(2)	162.7
O71-H71x…O21	0.93	1.67	2.591(2)	167.9
O81-H81x…O11	0.91	1.68	2.5831(19)	173.9
O91-H91x…O31	0.92	1.69	2.6144(19)	177.5
O161-H16x…O23	0.94	1.89	2.778(2)	156.7
O171-H17x…O33	0.95	1.83	2.756(2)	163.0

Symmetry operations used to generate equivalent atoms: a) x+1, y, z; b) x-1, y, z.

Table S3. Close π-π contacts (<4 Å)

π-Rings	**Centroid…Centroid**	**Mean plane intersects (°)**	**Offset angle (°)**
[Fe^{II}(**adpt**)$_2$(C$_{16}$SO$_3$)$_2$]			
N21-C25(coordinated pyridine)…N21-C25(coordinated pyridine)	3.5944(18)	0	20.0
N21-C25(coordinated pyridine)…N4-C12 (non-coordinated pyridine)	3.711(2)	5.6	21.3
[Co^{II}(**adpt**)$_2$(CH$_3$OH)$_2$](C$_{16}$SO$_3$)$_2$·1.33CH$_3$OH			
none present			

Table S4. Close anion-π contacts (centroid…non-coordinated anion < 3.3 Å)

	O…Centroid (Å)	**Mean plane…centroid…O angle (°)**	**S-O…centroid angle (°)**
O11…N2-C7 (coordinated triazole)	2.8878(17)	86.1	126.03(8)
O21…N22-C27 (coordinated triazole)	2.9340(18)	85.3	127.23(8)
O31…N42-C47 (coordinated triazole)	2.9631(17)	86.0	125.02(8)